An interesting effect of ring conformation and strain was observed for the (ethylenediaminetetracetato)cobalt(III) ([Co(EDTA)]$^-$) chelate.[25] This chelate contains two types of glycinate-like chelate rings: one (in-plane rings) is strained and bent. The other type of rings (out-of-plane rings) is planar and strain-free. The two kinds of chelate rings undergo H–D exchange of their methylene groups with different rates: the planar nonstrained rings undergo the exchange much more readily than do the nonplanar strained rings. It was suggested that this difference in reactivity originates in the large energy required by the bent rings in order to become a planar enolate ion.[25]

Another example of differentiation of reactivity caused by flexibility variation of chelate rings, which affects their ability to assume a planar enolate intermediate is demonstrated by Co(III) chelates of aspartic acid, where the amino acid is a tridentate ligand.[19b] Two chelate rings are formed: a six-membered ring, which is relatively flexible, and a five-membered ring, which is less flexible, because of its smaller size and because of the coordination of the side chain. The 3-methylene protons of the six-membered ring exchange slowly with deuterium, whereas the 2-methyne proton of the five-membered ring exchanges with deuterium much more slowly, probably concurrent with opening of the six-membered ring.

Acknowledgment. This research was supported by the Technion VPR Fund-The M. R. Saulson Research Fund. We thank Johnson Matthey Chemicals Ltd. for the loan of $RuCl_3$.

Registry No. $(NH_3)_5RuNH_2CH_2CON(CH_3)CH_2COOH^{3+}$, 108743-46-0; $(NH_3)_4RuNH_2CH_2CON(CH_3)CH_2COOH^{3+}$, 108743-47-1; $(NH_3)_4RuNH_2CH_2CONH_2^{3+}$, 85320-45-2; $(NH_3)_4RuNH_2CH_2CONHCH_2COOH^{3+}$, 85335-33-7; D_2, 7782-39-0.

(25) (a) Terrill, J. B.; Reilley, C. N. *Inorg. Chem.* **1966**, *5*, 1988–1996. (b) Williams, D. H.; Busch, D. H. *J. Am. Chem. Soc.* **1965**, *87*, 4644–4645.

Contribution from the Department of Chemistry, The University of Houston—University Park, Houston, Texas 77004, Laboratoire de Synthèse et d'Electrosynthèse Organométallique Associé au CNRS (UA 33), Faculté des Sciences "Gabriel", Université de Dijon, 21100 Dijon, France, and Laboratoire de Chimie-Physique Générale, Université Mohammed V, Rabat, Morocco

Synthesis, Electrochemistry, and Spectroelectrochemistry of Thallium(III) Porphyrins. Redox Properties of Five-Coordinate Ionic and σ-Bonded Complexes

K. M. Kadish,*[1a] A. Tabard,[1a] A. Zrineh,[1b,c] M. Ferhat,[1c] and R. Guilard*[1b]

Received December 11, 1986

The synthesis and physicochemical characterization of 10 different metal–carbon σ-bonded thallium porphyrins are reported, and these data are compared to those of two different chlorothallium(III) porphyrins. The ligands σ-bonded to the thallium octaethyl- and tetraphenylporphyrin complexes were CH_3, C_6H_5, p-$CH_3OC_6H_4$, C_6F_4H, and C_6F_5. Each neutral complex was characterized by ^1H NMR, IR, and UV–visible spectroscopy and electrochemistry. Spectroelectrochemistry and ESR were used to characterize each oxidized and reduced complex. The singly and doubly oxidized Tl(III) complexes containing σ-bonded alkyl or aryl groups were stable. The electrooxidations were reversible, and the formation of a π radical cation in the first electron abstraction was observed by ESR spectroscopy. The electroreduction was also porphyrin ring centered, but the generated anion radical stability varied according to the nature of the axial and equatorial ligands. Spectroscopic data suggest the formation of a transient monothallium(I) porphyrin complex before demetalation, but the ultimate products of electroreduction were the reduced free-base porphyrin and a species that spectroscopically resembled a bis(thallium(I)) porphyrin.

Introduction

There are only two reports in the literature on thallium porphyrin electrochemistry. Fuhrhop, Kadish, and Davis demonstrated that (OEP)TlOH undergoes a reversible one-electron reduction in Me_2SO and two reversible one-electron oxidations in butyronitrile.[2] These reactions were postulated to involve formation of porphyrin π radical anions and π radical cations, but no spectroscopic monitoring of the products was reported. A later investigation of (OEP)Tl($OCOCF_3$) and (TPP)Tl($OCOCF_3$) demonstrated that these two compounds could be reduced by two steps in DMF.[3] The first reduction occurred at $E_{1/2} = -0.35$ V for the tetraphenylporphyrin (TPP) and at −0.47 V for the octaethylporphyrin (OEP). Both reactions involved an initial two-electron addition, which was followed by demetalation of the complex. Formation of an intermediate Tl(I) porphyrin was postulated,[3] but this species was not spectroscopically characterized nor was an overall reduction mechanism proposed. In addition, no information was given as to the oxidative behavior of these two Tl(III) complexes.

In the present paper we present the synthesis, electrochemistry, and solution characterization of (OEP)TlCl, (TPP)TlCl, and 10 different (P)Tl(R) complexes where R is a σ-bonded C_6F_5, C_6F_4H, p-$CH_3OC_6H_4$, C_6H_5, or CH_3 group and P is TPP or OEP. Until recently, the electrochemistry of σ-bonded porphyrins was limited to complexes of iron and cobalt.[4,5] However, it is now known that the σ-bonded alkyl complexes of indium[6,7] and gallium[8] can be oxidized by a single-electron-transfer step and that rapid cleavage of the metal–carbon bond may[6] or may not[7] occur depending upon the nature of the σ-bonded group. Electrochemical and spectroscopic data indicate that the least stable $[(P)In(R)]^{\bullet+}$ and $[(P)Ga(R)]^{\bullet+}$ complexes are those with R groups having the largest σ-bonding character.[6-8] Oxidized In(III) and Ga(III) porphyrins with σ-bonded aryl groups rapidly decompose to give the ionic In(III) or Ga(III) porphyrin species in solution. In contrast, oxidized In(III) porphyrins with σ-bonded perfluoroaryl groups are quite stable[7] and electron abstraction from the neutral complex can be characterized as involving the porphyrin π ring system.[7] As will be shown in this study, the oxidations of both σ-bonded alkylthallium and σ-bonded arylthallium porphyrins are reversible and a characterization of the stable singly and doubly

(1) (a) University of Houston. (b) Université de Dijon. (c) Université Mohammed V.
(2) Fuhrhop, J.-H.; Kadish, K. M.; Davis, D. G. *J. Am. Chem. Soc.* **1973**, *95*, 5140.
(3) Giraudeau, A.; Louati, A.; Callot, H. J.; Gross, M. *Inorg. Chem.* **1981**, *20*, 769.
(4) Kadish, K. M. *Prog. Inorg. Chem.* **1986**, *34*, 435–605.
(5) Guilard, R.; Lecomte, C.; Kadish, K. M. *Struct. Bonding (Berlin)*, in press.
(6) Kadish, K. M.; Boisselier-Cocolios, B.; Cocolios, P.; Guilard, R. *Inorg. Chem.* **1985**, *24*, 2139.
(7) Tabard, A.; Guilard, R.; Kadish, K. M. *Inorg. Chem.* **1986**, *25*, 4277.
(8) Kadish, K. M.; Boisselier-Cocolios, B.; Coutsolelos, T.; Mitaine, P.; Guilard, R. *Inorg. Chem.* **1985**, *24*, 4521.

0020-1669/87/1326-2459$01.50/0

Table I. Characteristics of Reactions and Elemental Analyses of the Investigated (P)Tl(R) Complexes

porphyrin,[a] P	axial ligand, R	recrystn solvent[b]	yield, %	mol formula	anal., %[c] C	H	N	F	Tl
OEP	C_6F_5	A	71	$C_{42}H_{44}N_4F_5Tl$	55.6 (55.78)	4.8 (4.91)	5.9 (6.19)	9.5 (10.51)	21.8 (22.60)
	C_6F_4H	A	65	$C_{42}H_{45}N_4F_4Tl$	56.9 (56.92)	5.2 (5.13)	6.1 (6.32)	8.3 (8.58)	21.9 (23.06)
	p-$CH_3OC_6H_4$	A	71	$C_{43}H_{51}N_4OTl$	61.3 (61.17)	6.0 (6.10)	6.8 (6.63)		24.4 (24.21)
	C_6H_5	A	79	$C_{42}H_{49}N_4Tl$	62.6 (61.95)	6.1 (6.08)	6.7 (6.88)		24.6 (25.10)
	CH_3	A	82	$C_{37}H_{47}N_4Tl$	58.9 (59.08)	6.5 (6.31)	7.5 (7.44)		26.7 (27.17)
TPP	C_6F_5	A	57	$C_{50}H_{28}N_4F_5Tl$	60.9 (61.02)	2.9 (2.87)	5.6 (5.69)	8.9 (9.65)	20.4 (20.77)
	C_6F_4H	A	62	$C_{50}H_{29}N_4F_4Tl$	63.1 (62.15)	3.4 (3.03)	5.0 (5.80)	7.0 (7.87)	19.2 (21.15)
	p-$CH_3OC_6H_4$	B	64	$C_{51}H_{35}N_4OTl$	66.5 (66.27)	3.7 (3.82)	6.0 (6.06)		22.1 (22.11)
	C_6H_5	B	77	$C_{50}H_{33}N_4Tl$	67.2 (67.15)	3.8 (3.73)	6.2 (6.26)		22.8 (22.86)
	CH_3	C–D (1/1)	44	$C_{45}H_{31}N_4Tl$	64.2 (64.95)	3.6 (3.76)	6.2 (6.73)		23.7 (24.56)

[a] Abbreviations used: OEP = octaethylporphyrin; TPP = tetraphenylporphyrin. [b] Legend: A = toluene; B = dichloroethane; C = chloroform; D = heptane. [c] Calculated values are given in parentheses.

oxidized Tl(III) species is possible.

Experimental Section

Chemicals. Synthesis of the σ-bonded alkyl- and arylthallium porphyrins was carried out under an argon atmosphere. All common solvents were thoroughly dried in an appropriate manner and were distilled under argon prior to use. (OEP)TlCl and (TPP)TlCl were obtained by metalation of $(OEP)H_2$ and $(TPP)H_2$ with $TlCl_3$ in boiling *N,N*-dimethylformamide.[9] Reagent grade methylene chloride (CH_2Cl_2, Fisher) and benzonitrile (PhCN, Aldrich) were used for the electrochemical studies and were distilled from P_2O_5 prior to use. Tetrabutylammonium hexafluorophosphate ($(TBA)PF_6$) was purchased from Alfa and was recrystallized from ethyl acetate–hexane mixtures prior to use.

An early synthesis of $(P)Tl(CH_3)$ involved treatment of the free-base porphyrin with bis(acetato)methylthallium(III), $Tl(CH_3)(OAc)_2$.[10,11] In the present study, the (P)Tl(R) complexes were prepared by the action of an organomagnesium compound on (P)TlCl. A detailed procedure for this preparation is given below.

General Procedure for Preparation of (P)Tl(R) Where R = C_6F_5, C_6F_4H, p-$CH_3OC_6H_4$, C_6H_5 or CH_3. One equivalent of alkyl- or arylmagnesium bromide was added to (P)TlCl in 200 mL of tetrahydrofuran. The reaction mixture was kept at room temperature for the methyl derivative whereas the solution was refluxed for the other compounds. The reaction was monitored by UV–visible spectroscopy and was stopped after about 1 h. The reaction mixture was hydrolyzed with 50 mL of water and extracted three times with methylene chloride (200 mL). The organic layer was washed with water until neutrality and then dried over $MgSO_4$. After filtration, the organic solution was taken to dryness under reduced pressure by rotary evaporation. The obtained product was recrystallized from toluene or other solvents (see Table I for solvent of recrystallization) and gave a yield close to 70%.

Instrumentation. Elemental analyses were performed by the "Service de Microanalyse" of the CNRS. ^1H NMR spectra at 400 MHz were recorded on a Bruker WM 400 spectrometer of the Cerema ("Centre de Résonance Magnétique de l'Université de Dijon"). Spectra were measured from solutions of 5 mg of complex in C_6D_6 with tetramethylsilane as internal reference. ESR spectra were recorded at 115 K on a IBM Model ER 100 D spectrometer equipped with a microwave ER-040-X bridge and an ER 080 power supply. The g values were measured with respect to diphenylpicrylhydrazyl (g = 2.0036 ± 0.0003). Infrared spectra were obtained on a Perkin-Elmer 580 B apparatus. Samples were prepared as a 1% dispersion in CsI pellets. Electronic absorption spectra were recorded on a Perkin-Elmer 559 spectrophotometer, an IBM Model 9430 spectrophotometer, or a Tracor Northern 1710 holographic optical spectrophotometer–multichannel analyzer.

(9) Buchler, J. W. In *The Porphyrins*; Dolphin, D., Ed.; Academic: New York, 1978; Vol. I, Chapter 10, and references therein.
(10) Henrick, K.; Matthews, R. W.; Tasker, P. A. *Inorg. Chem.* **1977**, *16*, 3293.
(11) Brady, F.; Henrick, K.; Matthews, R. W. *J. Organomet. Chem.* **1981**, *210*, 281.

Table II. IR Data of the Investigated (P)Tl(R) Complexes (CsI Pellets)

porphyrin, P	R group	ν_{Tl-C}, cm^{-1}	ν_{Tl-Cl}, cm^{-1}
OEP	Cl^-		278
	C_6F_5	348	
	C_6F_4H	348	
	p-$CH_3OC_6H_4$	513	
	C_6H_5	435	
	CH_3	470	
TPP	Cl^-		290
	C_6F_5	350	
	C_6F_4H		
	p-$CH_3OC_6H_4$	510	
	C_6H_5	440	
	CH_3	480	

Cyclic voltammetry measurements were obtained with the use of a three-electrode system. The working electrode was a platinum button, and the counter electrode was a platinum wire. A saturated calomel electrode (SCE) was used as reference electrode and was separated from the bulk of the solution by a fritted-glass bridge. A BAS 100 electrochemical analyzer connected to a Houston Instruments HIPLOT DMP-40 plotter was used to measure the current–voltage curves.

Controlled-potential electrolysis was performed with an EG&G Model 173 potentiostat or a BAS 100 electrochemical analyzer. Both the reference electrode and the platinum-wire counter electrode were separated from the bulk of the solution by means of a fritted-glass bridge. Thin-layer spectroelectrochemical measurements were performed with an IBM EC 225 voltammetric analyzer coupled with a Tracor Northern 1710 holographic optical spectrophotometer–multichannel analyzer to give time-resolved spectral data. The utilized optically transparent platinum thin-layer electrode (OTTLE) has been described in a previous publication.[12]

Results and Discussion

Characterization of Neutral (P)TlCl and (P)Tl(R) Complexes. Infrared spectroscopic data for the Tl–Cl and Tl–C vibrations of each (P)TlCl or (P)Tl(R) complex are summarized in Table II. The characteristic ν_{Tl-Cl} vibration of (P)TlCl appears at 278 cm^{-1} (OEP complex) or 290 cm^{-1} (TPP complex). The C–F stretching modes of the perfluoroaryl derivatives appear in the frequency range 702–1475 cm^{-1} and are similar to frequencies reported for $(P)In(C_6F_5)$ and $(P)In(C_6F_4H)$.[7] At higher wavenumbers (1504–1633 cm^{-1}) the absorption bands are due to the ring vibrations.

Coordination of an alkyl or aryl group to the thallium metal gives a vibration in the range of 348–513 cm^{-1} (see Table II).

(12) Lin, X. Q.; Kadish, K. M. *Anal. Chem.* **1985**, *57*, 1498.

Table III. Maximum Absorbance Wavelengths (λ_{max}, nm) and Corresponding Molar Absorptivities ($10^{-3}\epsilon$, M^{-1} cm^{-1}) for Neutral (TPP)TlCl and (TPP)Tl(R) Complexes in C_6H_6

axial ligand, R	λ_{max}, ($10^{-3}\epsilon$) band I	B(1,0)	band II or B(0,0)	Q(2,0)	Q(1,0)	Q(0,0)	ϵ(II)/ϵ(I)
Cl^-		sh	434 (360.5)	520 (2.7)	566 (13.6)	608 (8.5)	
C_6F_5	336 (18.0)	417 (36.1)	438 (576.9)	531 (4.2)	577 (18.6)	620 (16.2)	32.0
C_6F_4H	335 (17.4)	417 (40.5)	438 (462.8)	530 (2.6)	576 (14.0)	622 (11.8)	26.6
p-$CH_3OC_6H_4$	341 (24.6)	424 (63.5)	444 (447.6)	544 (3.9)	585 (13.7)	626 (16.1)	18.2
C_6H_5	341 (28.7)	424 (57.3)	444 (493.8)	543 (3.9)	587 (15.0)	626 (17.7)	17.2
CH_3	340 (30.1)	424 (58.2)	444 (456.3)	542 (3.6)	588 (15.1)	625 (16.8)	15.2

Table IV. Maximum Absorbance Wavelengths (λ_{max}, nm) and Corresponding Molar Absorptivities ($10^{-3}\epsilon$, M^{-1} cm^{-1}) for Neutral (OEP)TlCl and (OEP)Tl(R) Complexes in C_6H_6

axial ligand, R	λ_{max} ($10^{-3}\epsilon$) band I	B(1,0)	band II or B(0,0)	Q(2,0)	Q(1,0)	Q(0,0)	ϵ(II)/ϵ(I)
Cl^-		sh	418 (225.7)	498 (2.1)	545 (11.8)	582 (10.5)	
C_6F_5	352 (33.5)	404 (46.1)	426 (335.2)	507 (1.4)	551 (18.3)	588 (10.7)	10.0
C_6F_4H	352 (29.5)	404 (38.1)	426 (277.4)	508 (1.3)	553 (15.3)	588 (8.8)	9.4
p-$CH_3OC_6H_4$	353 (40.6)	411 (57.6)	435 (259.8)	500 (2.0)	559 (17.2)	594 (5.6)	6.4
C_6H_5	355 (35.1)	412 (40.6)	435 (236.1)	500 (1.4)	559 (16.1)	595 (5.7)	6.7
CH_3	352 (38.9)	413 (43.7)	436 (232.3)	500 (1.4)	561 (17.2)	596 (5.8)	6.0

Comparison of these data with data on other organometallic thallium complexes[13-15] suggests that this vibration can be attributed to the ν_{Tl-C} mode. The other vibration modes observed with the (P)Tl(C_6H_5) and (P)Tl(p-$CH_3OC_6H_4$) complexes are similar to those of previously described thallium–aryl derivatives.[13]

Molar absorptivities of each (P)TlCl and (P)Tl(R) complex in C_6H_6 are summarized in Tables III and IV. The spectra of (P)TlCl compounds are classified as "normal" porphyrin electronic absorption spectra.[16,17] The σ-bonded thallium–carbon derivatives have UV–visible spectra that contain an additional blue-shifted band (band I), which is located between 335 and 355 nm. The spectral shape of the (P)Tl(R) species is analogous to that of the (P)In(R) and (P)Ga(R) complexes,[6-8] which belong to the hyper class.[17]

The ϵ(II)/ϵ(I) ratio of (P)Tl(R) can be correlated with the electron-donor properties of the σ-bonded R group.[6] The largest ϵ(II)/ϵ(I) ratio is obtained for (P)Tl(R) complexes with R = C_6F_5 and C_6F_4H while the smallest is for complexes with R = CH_3. These trends with change in the R group parallel the change of electron density on the porphyrin macrocycle that is induced by the axial ligand.

^{1}H NMR Spectroscopy. Table V summarizes ^{1}H NMR data for each (P)TlCl and (P)Tl(R) complex. No dramatic change in the porphyrin chemical shifts is observed as a function of the axial ligand. Also, the chemical shifts of the σ-bonded alkyl- or arylthallium complexes are more positive than those of (P)TlCl. Such a result is not observed for the gallium[8,20] and indium[6,19] series.

More positively charged central metal ions reduce the electron density on the porphyrin macrocycle and thus deshield the porphyrin protons.[18] The porphyrin electron density is also dependent on the electron-withdrawing properties of the axial ligand, and the meso proton chemical shift of (OEP)Tl(R) varies with the axial ligand, R, as

$$CH_3 < p\text{-}CH_3OC_6H_4 < C_6H_5 < C_6F_4H < C_6F_5$$

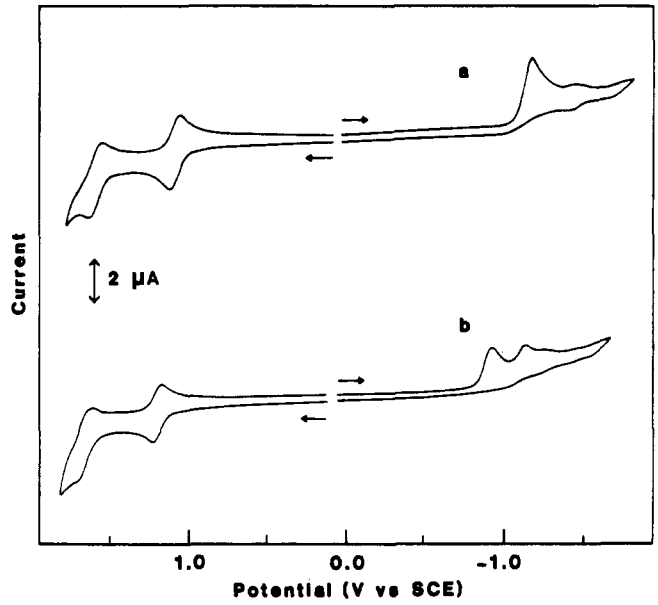

Figure 1. Cyclic voltammograms of (a) (OEP)TlCl and (b) (TPP)TlCl in CH_2Cl_2 containing 0.1 M (TBA)PF_6 (scan rate 100 mV/s).

The fact that the central metal atom of (P)Tl(R) is a heavy metal appears to be more important in influencing deshielding than the electron-donor or -acceptor properties of the axial ligand. Indeed, only the perfluoroaryl complexes of (P)In(R) have porphyrin proton signals more deshielded than those of (P)InCl.[7] The porphyrin proton resonances of (P)Ga(R) do not depend upon the electron-donor ability of the axial ligand.[8] This is in contrast to the case for (P)Tl(R), where the porphyrin electron density appears to be very sensitive to the nature of the axial ligand (alkyl, aryl, or ionic group). The perpendicular metal displacement from the porphyrin mean plane may induce this result.

As reported[21] in the literature, ^{1}H–^{203,205}Tl couplings are observed (see Table V) but only between Tl(III) and the meso or pyrrolic proton of the porphyrin macrocycle and the axial ligand proton. The magnitude of the coupling varied with the proton–thallium distance. The p-methoxy group does not show coupling, and there is no apparent influence of the porphyrin macrocycle on the coupling constant of the axial ligand proton. In contrast, the meso H–Tl and pyrrolic H–Tl couplings are largest with

(13) Nakamoto, K. *Infrared and Raman Spectra of Inorganic and Coordination Compounds*, 3rd ed.; Wiley: New York, 1978; p 372, and references therein.
(14) Goggin, P. L.; Woodward, L. A. *Trans. Faraday Soc.* **1960**, *56*, 1591.
(15) Deacon, G. B.; Green, J. H. S. *Spectrochim. Acta, Part A* **1968**, *24A*, 885.
(16) Abraham, R. J.; Barnett, G. H.; Smith, K. M. *J. Chem. Soc., Perkin Trans. 1* **1973**, 2142.
(17) Gouterman, M. In *The Porphyrins*; Dolphin, D., Ed.; Academic: New York, 1978; Vol. III, Chapter 1, and references therein.
(18) Sheer, H.; Katz, J. J. In *Porphyrins and Metalloporphyrins*; Smith, K. M., Ed.; Elsevier: Amsterdam, 1975; Chapter 10.
(19) Cocolios, P.; Guilard, R.; Fournari, P. *J. Organomet. Chem.* **1979**, *179*, 311.
(20) Coutsolelos, A.; Guilard, R. *J. Organomet. Chem.* **1983**, *253*, 273.
(21) Janson, T. R.; Katz, J. J. In *The Porphyrins*; Dolphin, D., Ed.; Academic: New York, 1978; Vol. IV, Chapter 1, and references therein.

Table V. ^{1}H NMR Data[a] of (P)TlCl and (P)Tl(R)

				protons of R^1			protons of R^2			protons of R		
P	R	R^1	R^2		mult/intens	δ^b		mult/intens	δ^b	mult/intens	δ^b	
OEP	Cl^-	H	C_2H_5	meso H	d/4	10.33 (39)	β-CH_3	t/24	1.79			
							α-CH_2	m/8	3.87			
							α'-CH_2	m/8	3.97			
	C_6F_5	H	C_2H_5	meso H	d/4	10.47 (18)	β-CH_3	t/24	1.87			
							α-CH_2	br/8	3.98			
							α'-CH_2	m/8	4.05			
	C_6F_4H	H	C_2H_5	meso H	d/4	10.45 (17)	β-CH_3	t/24	1.85	*p*-H	br/1	4.65
							α-CH_2	br/8	3.97			
							α'-CH_2	m/8	4.05			
	p-$CH_3OC_6H_4$	H	C_2H_5	meso H	s/4	10.37	β-CH_3	t/24	1.85	*o*-H	d/2	2.90 (739)
							α-CH_2	m/8	3.95	*m*-H	d/2	5.05 (173)
							α'-CH_2	m/8	4.10	*p*-CH_3	s/3	2.31
	C_6H_5	H	C_2H_5	meso H	s/4	10.40	β-CH_3	t/24	1.84	*o*-H	d/2	3.19 (601)
							α-CH_2	m/8	3.94	*m*-H	d/2	5.41 (218)
							α'-CH_2	m/8	4.08	*p*-H	d/1	5.59 (71)
	CH_3	H	C_2H_5	meso H	s/4	10.36	β-CH_3	t/24	1.87		d/3	−3.93 (694)
							α-CH_2	m/8	3.98			
							α'-CH_2	m/8	4.14			
TPP	Cl^-	C_6H_5	H	*o*-H	m/8	7.98	pyrr H	d/8	9.03 (63)			
				m-H, *p*-H	m/12	7.42						
	C_6F_5	C_6H_5	H	*o*-H	d/4	8.05	pyrr H	d/8	9.14 (39)			
				o'-H	d/4	8.42						
				m-H, *p*-H	m/12	7.46						
	C_6F_4H	C_6H_5	H	*o*-H	d/4	8.05	pyrr H	d/8	9.12 (37)	*p*-H	br/1	4.89
				o'-H	d/4	8.32						
				m-H, *p*-H	m/12	7.45						
	p-$CH_3OC_6H_4$	C_6H_5	H	*o*-H	s/4	8.07	pyrr H	s/8	9.10	*o*-H	d/2	3.37 (611)
				o'-H	s/4	8.21				*m*-H	d/2	5.33 (173)
				m-H, *p*-H	m/12	7.44				*p*-CH_3	s/3	2.51
	C_6H_5	C_6H_5	H	*o*-H	s/4	8.05	pyrr H	s/8	9.08	*o*-H	d/2	3.94 (640)
				o'-H	s/4	8.17				*m*-H	d/2	5.67 (224)
				m-H, *p*-H	m/12	7.42				*p*-H	d/1	5.85 (80)
	CH_3	C_6H_5	H	*o*-H	s/4	8.02	pyrr H	s/8	9.08		d/3	−3.59 (692)
				o'-H	s/4	8.33						
				m-H, *p*-H	m/12	7.47						

[a] Spectra were recorded in C_6D_6 at 21 °C with $SiMe_4$ as internal reference; chemical shifts (δ) downfield from $SiMe_4$ are defined as positive. Legend: R^1 = porphyrin methinic group; R^2 = porphyrin pyrrolic group; R = axial ligand; P = porphyrin; s = singlet; d = doublet; t = triplet; q = quadruplet; m = multiplet; br = broad peak. [b] Values in parentheses are ^1H–$^{203,205}Tl$ coupling constants in Hz.

(P)TlCl and are not observed with (P)Tl(R) where R = CH_3, C_6H_5, or *p*-$CH_3OC_6H_4$. This property agrees with the earlier noted dependence of the porphyrin electron density on the nature of the axial ligand. Also, the interaction between the meso and pyrrolic protons and the thallium center is stronger when the axial ligand has some electron-withdrawing ability (Cl^-, C_6F_5, C_6F_4H).

The signals of ethyl groups on the octaethylporphyrin complexes show a multiplet for the methylenic protons resulting from an ABX_3 coupling with the methylic protons. This is similar to the case for complexes in the gallium or indium series and agrees with pentacoordination of the Tl(III) metal as well as an out-of-plane metal atom. Similarly, an inequivalence of the porphyrin plane is also observed for tetraphenylporphyrin complexes and the ortho protons of the porphyrin phenyl groups are nonequivalent.

Oxidation of (TPP)TlCl and (OEP)TlCl. Cyclic voltammograms of (OEP)TlCl and (TPP)TlCl in CH_2Cl_2 containing 0.1 M (TBA)PF_6 are illustrated in Figure 1. The potential differences $|E_{pa} - E_{pc}| = 60 \pm 5$ mV and $|E_p - E_{p/2}| = 60 \pm 5$ mV, as well as the ratio $i_{pa}/i_{pc} = 1$ and the constant $i_p/v^{1/2} = 1$, indicate that the oxidations involve diffusion-controlled one-electron transfers. The first oxidation occurs at $E_{1/2} = 1.15$ V for (TPP)TlCl and at 1.03 V for (OEP)TlCl, and the differences in half-wave potentials between the first and the second oxidations of these two complexes are 0.45 and 0.48 V, respectively (Table VI). These data are consistent with criteria suggesting oxidations involving the successive formation of a π radical cation and dication.[2,4] Reversible ring-centered oxidations are also obtained for (P)InCl and (P)GaCl,[8,22] and $E_{1/2}$ values for the first oxidation of all three group 13 complexes are similar.[6,8] However, the abstraction of a second electron occurs at more positive potentials for (P)TlCl

Table VI. Half-Wave Potentials (V vs. SCE) of (P)TlCl and (P)Tl(R) in CH_2Cl_2 Containing 0.1 M (TBA)PF_6 (Scan Rate 100 mV/s)

porphyrin, P	axial ligand, R	oxidn		redn	
		2nd	1st	1st	2nd
OEP	Cl^-	1.51	1.03	−1.19[a]	
	C_6F_5	1.35	0.88	−1.42	
	C_6F_4H	1.36	0.86	−1.43	
	p-$CH_3OC_6H_4$	1.23	0.76	−1.49	
	C_6H_5	1.23	0.76	−1.49	
	CH_3	1.14	0.71	−1.52[b]	
TPP	Cl^-	1.60	1.15	−0.91[a]	
	C_6F_5	1.44	0.98	−1.17	−1.58[b]
	C_6F_4H	1.45	0.97	−1.19	−1.60[b]
	p-$CH_3OC_6H_4$	1.37	0.85	−1.25	−1.66[b]
	C_6H_5	1.40	0.88	−1.23	−1.64[b]
	CH_3	1.29	0.81	−1.27	−1.69[b]

[a] Peak potential measured at 0.10 V/s. [b] Values of peak potentials, E_p, at a scan rate of 1.6 V/s.

(22) Kadish, K. M.; Cornillon, J.-L.; Cocolios, P.; Tabard, A.; Guilard, R. *Inorg. Chem.* **1985**, *24*, 3645.

Table VII. Maximum Absorbance Wavelengths (λ_{max}, nm) and Corresponding Molar Absorptivities ($10^{-3}\epsilon$, M^{-1} cm^{-1}) for Neutral, Reduced, and Oxidized (TPP)TlCl and (TPP)Tl(R) in PhCN Containing 0.3 M $(TBA)PF_6$

axial ligand, R	electrode reacn	λ_{max} ($10^{-3}\epsilon$)		
Cl^-	none	436 (437)	568 (20)	608 (14)
	1st oxidn	421 (55)	510 (11)	628 (11)
C_6F_5	none	441 (407)	576 (16)	617 (14)
	1st redn	465	760	
	1st oxidn	420 (107)	525 (7)	615 (10)
C_6F_4H	none	441 (415)	576 (16)	618 (14)
	1st redn	464 (75)	763 (14)	875 (9)
	1st oxidn	422 (131)	524 (9)	613 (13)
p-$CH_3OC_6H_4$	none	447 (430)	586 (21)	629 (23)
	1st redn	475 (85)	785 (15)	
	1st oxidn	434 (175)	525 (6)	611 (9)
C_6H_5	none	447 (467)	585 (17)	628 (20)
	1st redn	476 (99)	784 (15)	
	1st oxidn	433 (173)	520 (7)	620 (7)
CH_3	none	448 (448)	587 (17)	629 (20)
	1st redn	477	775	
	1st oxidn	438 (160)	519 (21)	630 (16)

Table VIII. Maximum Absorbance Wavelengths (λ_{max}, nm) and Corresponding Molar Absorptivities ($10^{-3}\epsilon$, M^{-1} cm^{-1}) for Neutral, Reduced, and Oxidized (OEP)TlCl and (OEP)Tl(R) in PhCN Containing 0.3 M $(TBA)PF_6$

axial ligand, R	electrode reacn	λ_{max} ($10^{-3}\epsilon$)		
Cl^-	none	418 (286)	544 (21)	580 (17)
	1st redn	438	647	818
	1st oxidn	402 (74)	658 (8)	
C_6F_5	none	426 (308)	551 (24)	587 (15)
	1st redn	442	641	817
	1st oxidn	409 (107)	673 (12)	
C_6F_4H	none	426 (234)	552 (20)	589 (13)
	1st redn	440 (41)	645 (9)	825 (5)
	1st oxidn	412 (109)	675 (7)	
p-$CH_3OC_6H_4$	none	434 (247)	559 (23)	592 (12)
	1st redn	453 (61)	650 (8)	835 (8)
	1st oxidn	416 (85)	687 (7)	
C_6H_5	none	434 (248)	560 (22)	593 (11)
	1st redn	454 (86)	650 (9)	837 (8)
	1st oxidn	418 (71)	689 (11)	
CH_3	none	436 (268)	560 (24)	594 (11)
	1st redn	455		
	1st oxidn	417 (69)	692 (15)	

and $E_{1/2}$ follows the sequence (P)GaCl < (P)InCl < (P)TlCl.

The UV–visible spectrum of electrooxidized (TPP)TlCl in PhCN is illustrated in Figure 2a. The singly oxidized species has a Soret band at 421 nm (compared to 436 nm for the neutral complex) and two bands of equal intensity at 510 and 628 nm. The oxidation of (OEP)TlCl leads to a species with a blue-shifted Soret band at 402 nm and a single Q band at 658 nm (Tables VII and VIII). Both Soret bands are reduced in intensity with respect to those of the neutral (P)TlCl complexes, and the shape of the electronic spectra suggests formation of a π cation radical for both (OEP)TlCl and (TPP)TlCl.[23] There is a complete reversibility of these oxidations on the thin-layer electrochemistry time scale.

A single ESR signal at $g = 2.00$ is obtained for oxidized (TPP)TlCl. In contrast, singly oxidized (OEP)TlCl gives an ESR spectrum with two well-resolved symmetrical signals. The g value is close to 2.00, and the calculated coupling constant is 46.4 G. The shape of the spectrum reflects a coupling of the unpaired electron with the nuclear spin of thallium ($I = {}^1/_2$). Only one coupling is obtained, despite the two thallium isotopes (^{203}Tl, 29.52%; ^{205}Tl, 70.48%). The coupling constant accounts for a small spin density on the thallium nucleus, suggesting that the electron is essentially localized on the macrocycle.

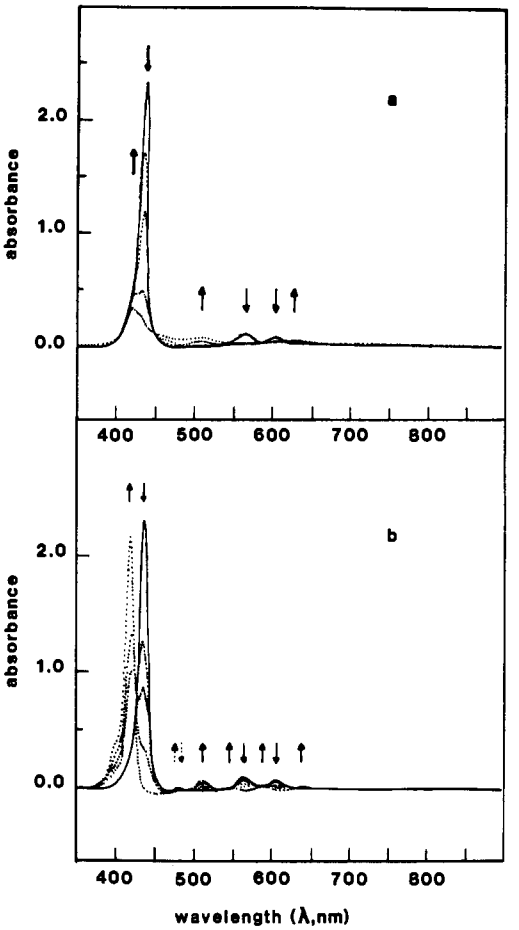

Figure 2. Time-resolved electronic absorption spectra taken during (a) oxidation of (TPP)TlCl and (b) reduction of (TPP)TlCl in PhCN containing 0.3 M $(TBA)PF_6$. The initial spectra are represented by a solid line while the intermediate and final spectra and represented by dashed lines.

ESR spectra of other (P)TlX complexes where X = ClO_4^- or CN^- are similar to spectra of (P)TlCl. Complexes in the thallium series[24] involve a σ–π spin polarization and a direct π interaction mechanism. For other group 13 metalloporphyrins, only a σ–π spin polarization mechanism is at the origin of the metal coupling.[8,22]

Reduction of (TPP)TlCl and (OEP)TlCl. The electroreduction of (P)TlCl differs from that of (P)GaCl and (P)InCl in that the last two complexes undergo reversible formation of radical anions and dianions in CH_2Cl_2.[6-8] A well-defined cathodic peak is obtained for the first reduction of (OEP)TlCl and (TPP)TlCl (Figure 1), but no reverse reoxidation waves are coupled to these reductions in the range of scan rates between 0.05 and 50 V/s.

The first reduction peak of (OEP)TlCl (see Figure 1a) has a value of $|E_p - E_{p/2}| = 65 \pm 6$ mV, consistent with a diffusion-controlled one-electron transfer. However, the lack of a reverse reoxidation peak for this process implies the occurrence of a fast chemical reaction following electron transfer. Also, the maximum peak currents for reduction of (OEP)TlCl are not self-consistent with currents for the reversible one-electron oxidation of the complex. The value of i_{pc} for reduction of (OEP)TlCl at −1.19 V is about 1.8 times higher than i_{pa} for oxidation at $E_{1/2} = 1.15$ V (see Figure 1a), thus suggesting the addition of two electrons in the reduction.

A similar electrochemical behavior is observed for (TPP)TlCl (see Table VI and Figure 1). The peak shape suggests a diffusion-controlled process, and the cathodic peak current is about 1.6 times higher than the oxidation peak current. The small

(23) Felton, R. H. In *The Porphyrins*; Dolphin, D., Ed.; Academic: New York, 1978; Vol. V, Chapter 3.

(24) Mengersen, C.; Subramanian, J.; Fuhrhop, J.-H.; Smith, K. M. *Z. Naturforsch., A: Phys., Phys. Chem., Kosmophys.* **1974**, *29A*, 1827.

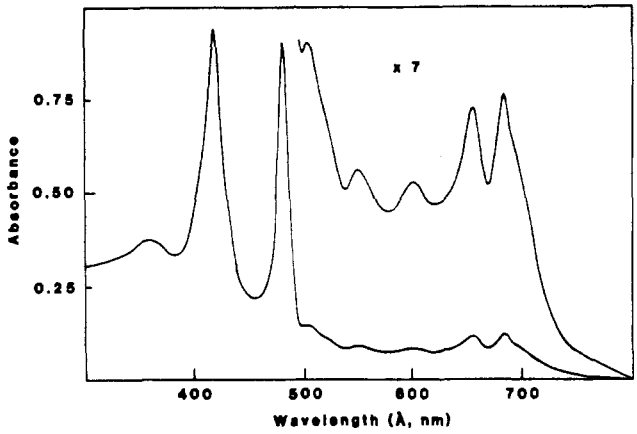

Figure 3. UV–visible spectrum recorded after bulk electrolysis of (TPP)TlCl in CH_2Cl_2 containing 0.1 M $(TBA)PF_6$ at −1.1 V vs. SCE.

reversible wave at $E_{1/2} = -1.22$ V is due to reduction of $(TPP)H_2$. Another peak at $E_{pc} = -1.12$ V can be attributed to reduction of a product resulting from the first electron step at −0.91 V.

Figure 2b shows representative time-resolved thin-layer spectra recorded during controlled-potential reduction of (TPP)TlCl in PhCN containing 0.3 M $(TBA)PF_6$. (TPP)TlCl has a Soret band at 436 nm and two Q bands at 568 and 608 nm (see Table VII). These three bands initially decrease during reduction while two new bands appear at 418 and 480 nm. However, as the reduction proceeds, the band at 418 nm increases in intensity while the band at 480 nm disappears. The final spectral product has bands at 514, 548, 588, and 645 nm and can be unambiguously attributed to $(TPP)H_2$. Also, the first reduction of $(TPP)H_2$ occurs at $E_{1/2} = -1.22$ V in CH_2Cl_2 and this wave is observed in cyclic voltammograms of (TPP)TlCl (see Figure 2b).

A similar spectral evolution is observed during controlled-potential reduction of (OEP)TlCl. An intermediate species with a Soret band at 480 nm is observed, but the intensities of the Q bands are too low to monitor. For this reason no assignment of the absorbing species was possible. However, it is clear that $(OEP)H_2$ is formed after several minutes of electrolysis.

Another spectral intermediate can also be characterized. This intermediate has a Soret band at 438 nm and Q bands at 647 and 818 nm. The intensities of these bands are lower than those of the starting material, and the red-shifted band is characteristic of a radical anion. All of the above data suggest that a Tl(III) radical anion is the first intermediate observed in reduction of the (P)TlCl complexes.

No ESR signal is observed after complete bulk electrolysis of (P)TlCl. The UV–visible spectra recorded just after the bulk electrolysis show formation of both free-base $(P)H_2$ and a second compound that has a Soret band at about 480 nm. Other bands appear at 364 and 684 nm for (TPP)TlCl (see Figure 3) and at 370 and 610 nm for (OEP)TlCl. Both intermediate spectra are clearly of the "hyper" type,[17] and these species are stable for at least several minutes under argon.

The first reduction of $(OEP)Tl(OCOCF_3)$ and $(TPP)Tl(OCOCF_3)$ has been proposed to correspond to a Tl(III) → Tl(I) process, which is followed by quantitative demetalation to give the corresponding free-base porphyrin.[3] However, Smith and Lai[25] have shown that Tl(I) porphyrins can be stabilized when two Tl(I) ions are coordinated to the porphyrin macrocycle.

The electronic absorption spectra of $(OEP)Tl_2$ and $(TPP)Tl_2$ are similar to spectra obtained in this study. This suggests that reductions of (OEP)TlCl and (TPP)TlCl lead to formation of unstable monothallium(I) derivatives which react to give the free-base porphyrin and a dithallium(I) porphyrin (see Figure 3). Thus, similarities between the literature spectra of dithallium porphyrins and spectra obtained in this study suggest that mono and bis Tl(I) complexes cannot be excluded as both intermediates and final products in the electroreduction of (P)TlCl.

(25) Smith, K. M.; Lai, J.-J. *Tetrahedron Lett.* **1980**, *21*, 433.

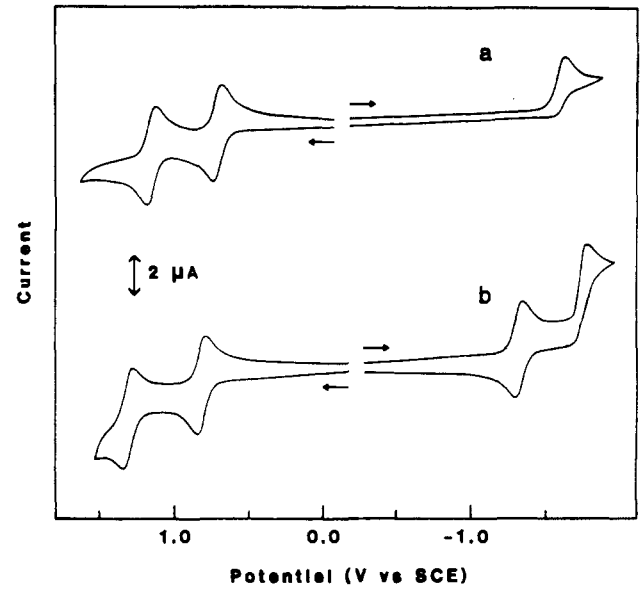

Figure 4. Cyclic voltammograms of (a) $(OEP)Tl(CH_3)$ and (b) $(TPP)Tl(CH_3)$ in CH_2Cl_2 containing 0.1 M $(TBA)PF_6$ (scan rate 100 mV/s).

Oxidation of (TPP)Tl(R) and (OEP)Tl(R). Half-wave potentials for oxidation and reduction of (P)Tl(R) in CH_2Cl_2 containing 0.1 $(TBA)PF_6$ are summarized in Table VI. Each of the (P)Tl(R) derivatives exhibit two reversible one-electron oxidations as shown for $(OEP)Tl(CH_3)$ and $(TPP)Tl(CH_3)$ in Figure 4.

A peak separation of $|E_{pa} - E_{pc}| = 60 \pm 5$ mV and a constant value of $i_p/v^{1/2}$ were obtained for each oxidation process, thus indicating a reversible one-electron-transfer reaction that is both diffusion-controlled and reversible. The number of electrons transferred in each step was also verified by controlled-potential coulometry.

The absolute potential difference between the first and second oxidation of each (P)Tl(R) complex varies between 0.43 mV and 0.52 V, which is comparable to values observed for the (P)TlCl complexes. These potential differences are slightly larger than those reported for other octaethylporphyrins,[2] but there is no doubt that the two oxidations are ring-centered.

Tables VII and VIII summarize time-resolved thin-layer spectroscopic data obtained during oxidation and reduction of (P)Tl(R). The spectra of oxidized and reduced $(OEP)Tl(C_6H_5)$ are represented in Figure 5. The abstraction of one electron from compounds in the (TPP)Tl(R) series leads to spectra with blue-shifted Soret bands of lower intensity, and two Q bands, which are located between 510 and 630 nm. A difference of 18 nm is observed between the Soret band of the oxidized compound with the weakest σ-bonding C_6F_5 group and that with the strongest σ-bonding CH_3 group. The spectral changes were reversible for all complexes except $(TPP)Tl(CH_3)$. The final spectral product in the oxidation of $(TPP)Tl(CH_3)$ has a Soret band at 422 nm, thus suggesting a cleavage of the thallium–CH_3 bond. However, this cleavage only occurred after 15 min of electrolysis in a thin-layer cell.

(OEP)Tl(R) undergoes spectral changes similar to those of (TPP)Tl(R) upon oxidation. The thin-layer voltammograms were reversible, and the spectra of the starting species could be regenerated by back-electrolysis. These spectral data show that the (OEP)Tl(R) complexes can be oxidized by a reversible one-electron transfer on the thin-layer time scale and that the formation of a porphyrin π cation radical is observed for each compound. Also, the oxidized $(OEP)Tl(CH_3)$ complex is less stable than the other oxidized compounds in the (OEP)Tl(R) series.

Abstraction of a second electron from $[(P)Tl(R)]^{\bullet+}$ leads to the reversible formation of a dication on the thin-layer electrochemical time scale, but a cleavage of the σ thallium–carbon bond does occur after several minutes. This instability is greater with compounds having a stronger σ-bonding character, and the most

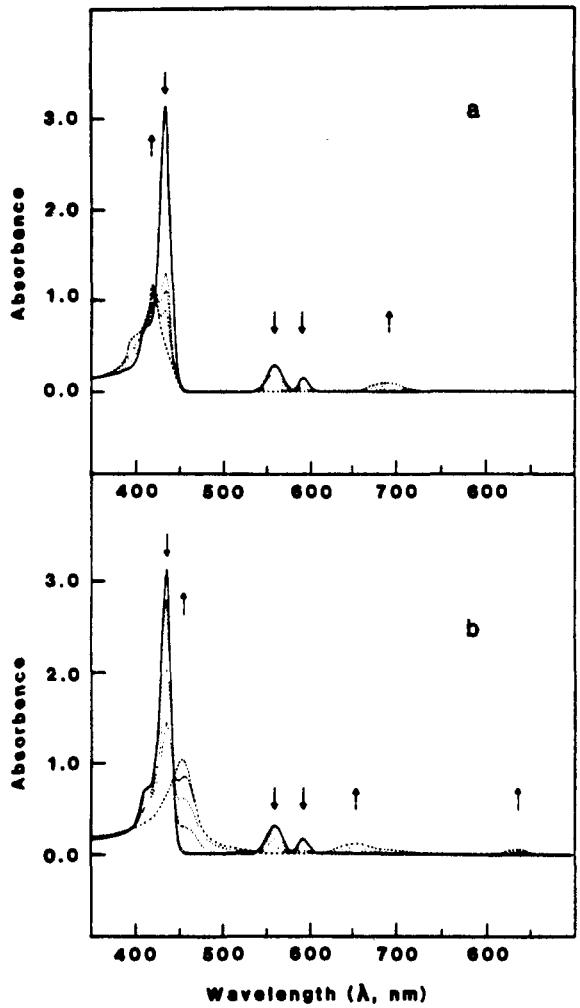

Figure 5. Time-resolved electronic absorption spectra taken during (a) oxidation of (OEP)Tl(C_6H_5) and (b) reduction of (OEP)Tl(C_6H_5) in PhCN containing 0.3 M (TBA)PF_6. The initial spectra are represented by a solid line while the intermediate and final spectra are represented by dashed lines.

rapid cleavage of the Tl–carbon bond is observed with complexes with a CH_3 axial ligand. Also, the doubly oxidized (OEP)Tl(R) derivatives are less stable than doubly oxidized (TPP)Tl(R) complexes.

ESR data measured at 120 K after complete bulk oxidation of (P)Tl(R) and (P)TlCl in CH_2Cl_2 containing 0.1 M (TBA)PF_6 are summarized in Table IX. The g factor is close to the free spin value of 2.0023 for each oxidized complex, and this result is consistent with the formation of a radical cation. The isotropic spectra consist of two well-defined signals for each compound. This is similar to the case for $[(OEP)TlCl]^+$ and is due to a coupling of the unpaired electron with the nuclear spin of thallium ($I = {}^1/_2$). No difference in coupling with the two isotopes is observed.

The ESR spectra of $[(P)Tl(R)]^{\bullet+}$ can be explained by a delocalization of spin onto the metal of the porphyrin and has been reported for other metalloporphyrins.[3,5,7,26-29] Direct π–π interaction of the thallium orbitals with the porphyrin π system has been proposed to account for the ^{205}Tl splitting.[24] The data in Table IX show that the coupling constant is dependent upon the nature of the axial ligand. In particular, the splitting for the alkyl or aryl (P)Tl(R) complexes is larger than the splitting for the perfluoroaryl (P)Tl(R) or (P)TlCl derivatives.

Table IX. ESR Data of Singly Oxidized and Reduced (P)TlCl and (P)Tl(R) Complexes in CH_2Cl_2 Containing 0.1 M (TBA)PF_6 at 120 K

	1st oxidn		1st redn	
compd	A, G	g	ΔH, G[a]	g
(OEP)TlCl	46.4	2.00		
(OEP)Tl(C_6F_5)	42.3	2.00	62.1	2.00
(OEP)Tl(C_6F_4H)	31.6	2.00	73.9	2.00
(OEP)Tl(p-$CH_3OC_6H_4$)	110.2	2.00	139.1	2.01
(OEP)Tl(C_6H_5)	107.5	2.01	121.0	2.00
(OEP)Tl(CH_3)	165.3	2.02	155.9	2.00
(TPP)TlCl		2.00		
(TPP)Tl(C_6F_5)	172.3	2.01	71.2	2.00
(TPP)Tl(C_6F_4H)	189.1	2.01	64.5	2.00
(TPP)Tl(p-$CH_3OC_6H_4$)	341.4	2.01	115.6	2.01
(TPP)Tl(C_6H_5)	350.8	2.01	114.9	2.00
(TPP)Tl(CH_3)	405.9	2.01	155.1	2.02

[a] ΔH is the derivative peak difference.

The NMR data unambiguously show that the thallium metal is out of the plane of the porphyrin ring, and this is confirmed by molecular structures of (TPP)TlCl and (TPP)Tl(CH_3).[10] The distances of the thallium ion from the mean plane of the four pyrrole nitrogens are 0.74 and 0.98 Å, for (TPP)TlCl and (TPP)Tl(CH_3), respectively. The coupling constants reflect this difference. The σ-bonded CH_3 complex has the largest splitting. Also, the distance of the thallium ion from the mean plane of the four pyrrole nitrogens is 0.69 Å in the (OEP)TlCl complex.[30] The same difference should be observed between other thallium–alkyl or thallium–aryl compounds in the (OEP)Tl(R) and (TPP)Tl(R) series, and the values of the coupling constants are in agreement with these structural differences. Thus, the decreased stability of the (P)Tl(CH_3) radical cation and dication agrees with ESR results, which show a large interaction of the thallium nucleus with the porphyrin π ring system.

The coupling constants summarized in Table IX reflect only a small unpaired electron density on the thallium ion. Thallium metal is expected to give an isotropic coupling constant of 7000 G,[24] and the observed splitting accounts for a spin density of about 0.45–5.80% on the thallium nucleus. Thus, the electron is essentially localized on the macrocycle ring.

Reduction of (TPP)Tl(R) and (OEP)Tl(R). One or two reductions are observed for (TPP)Tl(R) depending on the nature of the macrocycle. These reactions are represented by the cyclic voltammograms of (TPP)Tl(CH_3) and (OEP)Tl(CH_3) in Figure 4.

The potential differences $|E_p - E_{p/2}| = 60 \pm 5$ mV and $|E_{pa} - E_{pc}| = 60 \pm 5$ mV as well as the constant value $i_p/v^{1/2}$ for the first reduction indicate an electrochemically reversible one-electron transfer for complexes in the (TPP)Tl(R) series. Half-wave potentials for these reactions are summarized in Table VI. The potential difference between the first oxidation and the first reduction of (TPP)Tl(R) is 2.12 ± 0.04 V and agrees with the generally observed separation of 2.25 ± 0.15 V for a ring-centered oxidation and a ring-centered reduction.[2]

The second reduction of (TPP)Tl(R) occurs at potentials between $E_{1/2} = -1.58$ V and $E_{1/2} = -1.69$ V. At scan rates less than 200 mV/s the i_{pc}/i_{pa} ratio is larger than unity. However, at larger scan rates, the electron transfer appears reversible and the difference in $E_{1/2}$ between the first and the second reduction is 0.41 ± 0.01 V, suggesting two reductions at the porphyrin π ring system. The larger ratio of i_{pc}/i_{pa} that is obtained on longer time scales suggests a slow chemical reaction following electron transfer. At scan rates <50 mV/s the cathodic peak current for the second reduction is larger than the current for the first reduction. This is evident by normal pulse polarography, where the ratio of currents for these two processes is 1.9. Also, at all scan rates a reverse peak is invariably coupled to the first reduction. These

(26) Wolberg, A.; Manassen, J. *J. Am. Chem. Soc.* **1970**, *92*, 2982.
(27) Fajer, J.; Borg, D. C.; Forman, A.; Dolphin, D.; Felton, R. H. *J. Am. Chem. Soc.* **1970**, *92*, 3451.
(28) Fajer, J.; Borg, D. C.; Forman, A.; Adler, A. D.; Varodi, V. *J. Am. Chem. Soc.* **1974**, *96*, 1238.
(29) Fajer, J.; Borg, D. C.; Forman, A.; Felton, R. H.; Vehg, L.; Dolphin, D. *Ann. N.Y. Acad. Sci.* **1973**, *206*, 349.
(30) Cullen, D. L.; Meyer, E. F.; Smith, K. M. *Inorg. Chem.* **1977**, *16*, 1179.

observations indicate that a chemical reaction does not occur directly after the one-electron transfer but that there is the possibility to add a third electron to the starting complex.

The (OEP)Tl(R) derivatives have only one reduction in the potential range of methylene chloride (see Figure 4a). Half-wave potentials for this reduction vary between $E_{1/2} = -1.42$ V and $E_{1/2} = -1.52$ V depending on the axial ligand. The absolute potential difference between the first oxidation and the first reduction of (OEP)Tl(R) is 2.26 ± 0.04 V, in agreement with a ring-centered reduction in the first step.

A reversibility of the first reduction is observed for all (P)Tl(R) complexes where R = aryl group. However, the (OEP)Tl(CH_3) complex (represented in Figure 4a) has no reverse peak at 100 mV/s, and characteristics of this electron transfer are similar to those for the second reduction of (TPP)Tl(R).

Each (P)Tl(R) complex is reduced by either one or two one-electron transfers at −78 °C, and the formation of a Tl(I) porphyrin is possible by analogy with the (P)TlCl complexes. The wavelengths of maximum absorbance and the molar absorptivities for the reduced (P)Tl(R) complexes are given in Tables VII and VIII. The singly reduced (TPP)Tl(R) derivatives exhibit a red-shifted Soret band, which is located between 464 and 477 nm, and one or two Q bands.

The reduced (TPP)Tl(R) complexes have a red-shifted Soret band whose wavelength is dependent upon the electron-donor properties of the axial ligand. The reduced (OEP)Tl(R) complexes have one band in the visible region and a Soret band that ranges between 440 and 455 nm (see Figure 5b).

The reduced (P)Tl(C_6F_5) complex was not stable at long time scales, and only the wavelengths of maximum absorbance are reported in Tables VII and VIII. However, the thin-layer voltammograms were reversible and the spectrum of the starting species could be regenerated by back-electrolysis. A similar stability was observed for all of the complexes except those containing a σ-bonded CH_3 axial ligand.

Both (OEP)Tl(CH_3) and (TPP)Tl(CH_3) were unstable on the thin-layer voltammetry time scale after the addition of one electron and, similar to the case for (OEP)TlCl and (TPP)TlCl, an intermediate with a Soret band around 480 nm was observed. Demetalation also occurred to give the porphyrin free base as a final product. The resulting spectra indicate that the first electron transfer involves the porphyrin π ring system. The formation of a Tl(I) derivative can occur, but the size of the Tl(I) ion is incompatible with the core radius of the porphyrin, and this would lead to demetalation.[3]

The second reduction of (TPP)Tl(R) also leads to formation of $(TPP)H_2$ as an ultimate product. The singly reduced (P)Tl(R) derivatives are ESR-active, and the g values and peak differences (ΔH) are summarized in Table IX. The ESR data for compounds in the (TPP)Tl(R) and (OEP)Tl(R) series are comparable. However, the ΔH peak difference varied from 62 to 156 G as a function of the nature of the axial ligand.

For each $[(P)Tl(R)]^{\bullet-}$ compound, the g value is close to the free-spin g_e value of 2.0023. These results agree with spectroelectrochemical results, which suggest formation of a radical anion.[31,32] A small radical signal was also sometimes observed with a g value close to 2.00. This signal was not always present nor was its intensity constant, suggesting that this signal is due to a side product of the electroreduction.

The UV–visible spectra of the final reduction product show the existence of both the free-base porphyrin and a second stable complex that has a Soret band at 480 or 482 nm (depending on the nature of the porphyrin ring). This is similar to spectral data from reduced (P)TlCl and indicates a possible reaction between $(TPP)H_2$ and Tl(I) that leads to formation of a dithallium(I) porphyrin.

In summary, thallium porphyrins show the most unusual behavior of all group 13 metalloporphyrins. The oxidation of alkyl σ-bonded (P)Ga(R) and (P)In(R) porphyrins is followed by a metal–carbon bond cleavage, the rate of which depends upon the electron-donating properties of the axial ligand. Oxidized thallium complexes have a more stable σ bond, and the oxidation is unambiguously ring-centered. The Tl(III) ion is significantly out of the plane of the porphyrin macrocycle. No overlap occurs between the σ orbitals and the porphyrin HOMO orbitals; i.e., there is a great separation of their respective energy levels.

The thallium ion can be an electron acceptor, and the large size of Tl(I) is incompatible with complexation by the porphyrin macrocycle. Thus, a demetalation occurs after reduction. This is unlike the case for the gallium or indium complexes, which form stable anion radicals upon electroreduction.

Acknowledgment. The support of the National Science Foundation (Grant Nos. CHE-8515411 and INT-8413696) and the CNRS is gratefully acknowledged.

Registry No. (OEP)Tl(C_6F_5), 108150-25-0; (OEP)Tl(C_6F_4H), 108150-26-1; (OEP)Tl(p-$CH_3OC_6H_4$), 108150-27-2; (OEP)Tl(C_6H_5), 108167-04-0; (OEP)Tl(CH_3), 63848-52-2; (TPP)Tl(C_6F_5), 108150-28-3; (TPP)Tl(C_6F_4H), 108150-29-4; (TPP)Tl(p-$CH_3OC_6H_4$), 108150-30-7; (TPP)Tl(C_6H_5), 108150-31-8; (TPP)Tl(CH_3), 63848-50-0; (OEP)TlCl, 58167-68-3; (TPP)TlCl, 63848-51-1; $[(OEP)TlCl]^{\bullet+}(PF_6)^-$, 108150-33-0; $[(OEP)Tl(C_6F_5)]^{\bullet+}(PF_6)^-$, 108150-35-2; $[(OEP)Tl(C_6F_4H)]^{\bullet+}(PF_6)^-$, 108150-37-4; $[(OEP)Tl(p\text{-}CH_3OC_6H_4)]^{\bullet+}(PF_6)^-$, 108150-39-6; $[(OEP)Tl(C_6H_5)]^{\bullet+}(PF_6)^-$, 108150-41-0; $[(OEP)Tl(CH_3)]^{\bullet+}(PF_6)^-$, 108150-43-2; $[(TPP)TlCl]^{\bullet+}(PF_6)^-$, 108150-45-4; $[(TPP)Tl(C_6F_5)]^{\bullet+}(PF_6)^-$, 108150-47-6; $[(TPP)Tl(C_6F_4H)]^{\bullet+}(PF_6)^-$, 108150-49-8; $[(TPP)Tl(p\text{-}CH_3OC_6H_4)]^{\bullet+}(PF_6)^-$, 108150-51-2; $[(TPP)Tl(C_6H_5)]^{\bullet+}(PF_6)^-$, 108150-52-3; $[(TPP)Tl(CH_3)]^{\bullet+}(PF_6)^-$, 108150-53-4; $[(OEP)Tl(C_6F_5)]^{\bullet-}$, 108150-54-5; $[(OEP)Tl(C_6F_4H)]^{\bullet-}$, 108150-55-6; $[(OEP)Tl(p\text{-}CH_3OC_6H_4)]^{\bullet-}$, 108150-56-7; $[(OEP)Tl(C_6H_5)]^{\bullet-}$, 108150-57-8; $[(OEP)Tl(CH_3)]^{\bullet-}$, 108150-58-9; $[(TPP)Tl(C_6F_5)]^{\bullet-}$, 108150-59-0; $[(TPP)Tl(C_6F_4H)]^{\bullet-}$, 108150-60-3; $[(TPP)Tl(p\text{-}CH_3OC_6H_4)]^{\bullet-}$, 108150-61-4; $[(TPP)Tl(C_6H_5)]^{\bullet-}$, 108150-62-5; $[(TPP)Tl(CH_3)]^{\bullet-}$, 108150-63-6; C_6F_5MgBr, 879-05-0; C_6F_4HMgBr, 40586-92-3; p-$CH_3OC_6H_4MgBr$, 13139-86-1; C_6H_5MgBr, 100-58-3; CH_3MgBr, 75-16-1.

(31) Fajer, J.; Davis, M. S. In *The Porphyrins*; Dolphin, D., Ed.; Academic: New York, 1978; Vol. IV, Chapter 4.
(32) Felton, R. H.; Linschitz, H. *J. Am. Chem. Soc.* **1966**, *88*, 1113.